

Effect of growth conditions on the mechanical properties of lanthanum-gallium tantalate crystals

Mark V. Weintraub¹, Nina S. Kozlova¹, Evgeniya V. Zabelina¹, Mikhail I. Petrzhik¹

1 National University of Science and Technology MISiS, 4 Leninsky Prospekt, Moscow 119049, Russia

Corresponding author: Nina S. Kozlova (kozlova_nina@mail.ru)

Received 19 June 2020 ♦ Accepted 8 July 2020 ♦ Published 15 July 2020

Citation: Weintraub MV, Kozlova NS, Zabelina EV, Petrzhik MI (2020) Effect of growth conditions on the mechanical properties of lanthanum-gallium tantalate crystals. *Modern Electronic Materials* 6(2): 65–70. <https://doi.org/10.3897/j.moem.6.2.63731>

Abstract

The effect of growth conditions, anisotropy and polarity of specimens on the mechanical properties of lanthanum-gallium tantalate $\text{La}_3\text{Ta}_{0.5}\text{Ga}_{5.5}\text{O}_{14}$ single crystals grown in different atmospheres (argon (Ar), argon with oxygen addition ($\text{Ar}+(\lt 2\%)\text{O}_2$ and $\text{Ar}+(2\%)\text{O}_2$) and air) was studied. The test specimens for the measurements were cut perpendicularly to a 3rd order axis (*Z* cuts) and in polar directions perpendicular to a 2nd order axis (*Y* cuts). The polarity of the *Y* cut specimens was tested by piezoelectric response. The brittleness was evaluated by microindentation at 3, 5, 10 and 25 g loads. The brittleness proved to show itself at a 5 g and the higher loads regardless of growth atmosphere. Therefore microhardness tests were done at loads of within 3 g. The microhardness HV of the specimens was measured with an DM 8B Affri microhardness tester by Vickers methods. The hardness *H*, elastic modulus *E* and elastic recovery coefficient *R* were measured with a Berkovich pyramid on a CSM Nano-Hardness Tester using the instrumented indentation (nanoindentation) method. Growth atmosphere was shown to affect the mechanical properties of lanthanum-gallium tantalate crystals: crystals grown in an oxygen-free argon atmosphere had the lowest microhardness, hardness, elastic modulus and elastic recovery coefficient. The lowest microhardness was detected in *Z* cut specimens regardless of growth atmosphere. The mechanical properties of polar *Y* cuts proved to be anisotropic: the microhardness, hardness, elastic modulus and elastic recovery coefficient of these cuts were lower for positive cuts than for negative ones regardless of growth atmosphere. *Y* and *Z* cut langatate specimens grown in argon with less than two percent oxygen exhibited strong elastic modulus and elastic recovery coefficient anisotropy.

Keywords

langatate, single crystal, growth atmosphere, mechanical properties, microhardness test, instrumental indentation, microhardness, hardness, elastic modulus, elastic recovery coefficient, anisotropy.

1. Introduction

Improvement of the performance of piezoelectric devices requires prospective materials with a new gamut of properties including lanthanum-gallium tantalate $\text{La}_3\text{Ta}_{0.5}\text{Ga}_{5.5}\text{O}_{14}$ (**langatate**, **LGT**). Lanthanum-gallium tantalate crystals are non-centrosymmetrical trigonal symmetry 32 (L_33L_2) and hence they have piezoelectric properties, their piezoelectric moduli being

$d_{11} = 6.63 \times 10^{-12}$ C/N and $d_{14} = 5.55 \times 10^{-12}$ C/N [1]. They are not hygroscopic, nor pyro- or ferroelectric and do not exhibit phase transitions until the melting point [1–3]; and no data on twinning in these materials were found in literature.

Polar LGT cuts are successfully used today as working components of piezoelectric devices [4–6]. These sensors convert mechanical energy into electric one thus offering the possibility to manufacture pressure, temperature, vi-

bration, weight, flowrate etc. gages. Piezoelectric sensors are miniaturized and do not require external power sources, their stability against external factors depending mainly on the stability of the crystal component. The main advantage of LGT is the absence of piezoelectric modulus drift which makes them suitable for high temperature applications, e.g. pressure gages in internal combustion engines [7].

To fabricate a sensing element for use in pressure gages one should mechanically treat langatate crystals (cutting, polishing and grinding). How there are but scarce data on the mechanical properties of langatate crystals [8–11]. Langatate crystals have anisotropic microhardness but data of different reports scatter significantly (Table 1).

Table 1. Langatate microhardness data of different reports.

Growth atmosphere	Anneal	Color	Cut	Direction	Microhardness, GPa	Ref.
Ar+(1%) O ₂	Vacuum	No	Y54°	–	12.2	[8]
–	No	Orange	–	–	13.8	–
–	–	–	(11 $\bar{2}$ 0)	[1 $\bar{1}$ 00]	7.7±0.1	[9, 10]
–	–	–	–	[0001]	8.3±0.1	–
–	–	–	(11 $\bar{2}$ 0)	–	10.22	[11]
–	–	–	(10 $\bar{1}$ 0)	–	10.08	–
–	–	–	(0001)	–	8.77	–

Of greatest interest is the working polar cut perpendicular to a 2nd order axis ((10 $\bar{1}$ 0) or (01 $\bar{1}$ 0)) but data on the microhardness of this cut are available in only one work [11].

The optical and electrical parameters of langatate are known to depend largely on crystal growth atmosphere [12–18] but growth atmosphere was rarely specified in earlier works.

Working piezoelectric cuts of langatate crystals are polar [18] and hence the surface energy and microhardness of the cuts should differ. However crystal polarity was not taken into account in earlier reported tests.

Thus there is the need for a systematic study of the mechanical properties of lanthanum-gallium tantalate crystals including their polar cuts finding practical applications in sensing elements of high-temperature pressure gages.

2. Specimens and measurement methods

Z cut and polar Y cut specimens grown in different atmospheres were studied: argon (Ar), argon with oxygen (Ar + < 2 % O₂), argon with oxygen (Ar + 2 % O₂) and air.

Plate side polarity was tested by piezoelectric response. Vickers microhardness (*HV*) was tested at a constant dwell time (10 s) and load advancing speed (50 mm/s) on an automatic microhardness tester DM 8B (Affri, Italy) allowing measurements at small loads (1, 3, 5, 10 and 25 g). The hardness *H*, indentation elastic modulus *E_i* and elastic recovery coefficient *R* were measured and anisotropy and effect of growth atmosphere on the mechanical properties of langatate crystals were studied with a Berkovich pyramid [19] on a Nano-Hardness Tester (CSM Instr., Switzerland) using the instrumented indentation (nanoindentation) method.

3. Mechanical testing methods

Hardness measurements have a large number of research and technical applications although there is still a discussion regarding the physical sense of this parameter and correct evaluation methods [19, 20]. The fundamentals of the microhardness theory and evaluation methods were put forward by H.R. Hertz. Hardness is the property of surface layers to resist elastic and plastic deformation or fracture upon local indentation by a harder body (indenter) of a specific shape and size that does not acquire residual deformation [21].

The basics of the methods being considered is the analytical solution [22] of the so-called Hertz problem (1882) of mutual deformation of two hard balls upon their compression which was discussed in details earlier [23].

For Vickers microhardness testing (GOST 2999-75) [24] a tetrahedral pyramid with the vertex angle $\alpha = 136$ arc deg is pressed into material surface and the indentation diagonal length *d* is measured after indentation load removal. The Vickers hardness is calculated as the ratio of the load *P* to the pyramid indentation surface area *M*.

$$HV = \frac{P}{M} = \frac{2P \sin\left(\frac{\alpha}{2}\right)}{d^2} = 1,854 \frac{P}{d^2} \quad (1)$$

The conventional method of indenter and specimen interaction was justified for the case of negligibly small surface forces in comparison with the total interaction forces. For materials with a higher percentage of elastic deformation this method gives overestimated hardness [25]. The conventional hardness measurement method is not either suitable for hard and superhard materials because for small loads the imprint is so small that is often not visible under optical microscope whereas high loads cause cracking.

The advantage of instrumental indentation is determined by the use of high-precision resolution for the depth of indentation and the magnitude of the applied load, which reach nanoscale values, namely nanometers and nanoNewtons [26]. Nanoindentation has found growing applications in recent years for measuring hardness and elastic modulus of nearsurface layers. The indenter penetrates into material to a depth of tens to hundreds of nanometers and gives information on mechanical properties testing very small volumes of materials.

Indentation size is measured for the maximum indentation depth *h_m* in the assumption that the diamond indenter is not deformed upon indentation. Π curves are similar to tension curves at low deformations (Fig. 1). Π data are usually processed method described in [27] implying selection of parameters of a power function describing the experimental indentation depth vs applied load dependence.

Hardness is calculated as the ratio of the maximum load to the unrecovered indentation projection area and elastic modulus is determined based on the indentation

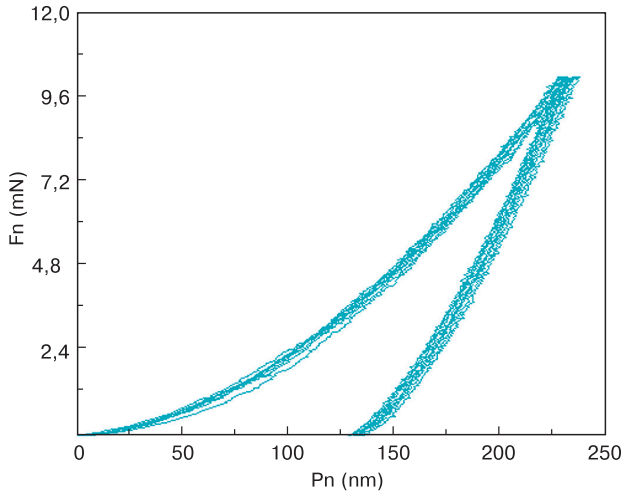


Figure 1. Typical experimentation II curves – family of 9 indentation curves of sample 2. F_n – applied load, mN, P_d – penetration depth, nm.

area and the contact stiffness as $S = dP/dh$ from the slope of the unloading curve upper third portion.

$$E = \frac{S}{2} \left(\frac{\pi}{A_p} \right)^{\frac{1}{2}} \quad (2)$$

where E is Young’s modulus, ν is Poisson’s ratio of the tested material, h_c is depth over which the indenter and specimen are in contact during the force application, A_p is projected (cross section) area of indenter h_c . Indenter penetration into material produces a complex stressed state in the vicinity of the contact area which is close to uniform compression, the in-depth propagating deformation having elastic (recoverable) and plastic (non-recoverable) components. This allows II to be used for retrieving information on hardness, Young’s modulus and elastic recovery coefficient in total deformation characterized by elastic recovery

$$R = \frac{h_{max} - h_p}{h_{max}}, \quad (3)$$

where h_{max} is maximum value of h , h_p is the permanent recovered indentation depth after removal of test force.

4. Experimental

Preliminary microhardness tests of Y cut langatate crystals grown in an Ar + < 2 % O_2 atmosphere were conducted. Langatate is a brittle crystal and therefore the indentation loads were small: 3, 5, 10 and 25 g. Figure 2 shows indentation photos.

With 3 g load indenter produces a clear imprint without visible cracks or cleaves (Fig. 2a). Increasing the indenter load to 5 g causes three cracks that can be seen on the indentation as extensions of indentation diagonals (Fig. 2b). The two longer cracks are extensions of the horizontal indenter diagonal and the third crack extends to beyond the vertical indentation diagonal. Further increase in the

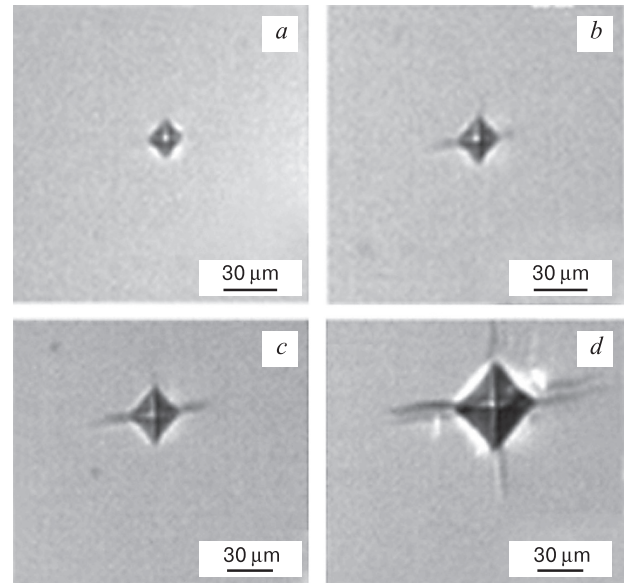


Figure 2. Indentation photos for different loads in Y cut langatate specimen grown in an Ar + < 2 % O_2 atmosphere: (a) 3 g, (b) 5 g, (c) 10 g and (d) 25 g

indenter load to 25 g causes development of these cracks (Fig. 2 c).

The brittleness of the material was evaluated following the method described earlier [29] on a five-point scale where each of the indentations is given a brittleness rate determined on an arbitrary scale (Table 2) taking into account the number and development pattern of cracks for a specific indentation. Microhardness data obtained with this method are considered correct if the brittleness rate of an indentation is within 2.

Table 2. Mean brittleness rate determination for microindentation method [27].

Mean brittleness rate	Indentation pattern
0	Indentation without visible cracks or cleaves
1	One small crack at indentation corner
2	One crack not coincident with indentation diagonal extension. Two cracks in adjacent indentation corners
3	Two cracks in opposite indentation corners. Three cracks in different indentation corners. Cleave at one indentation side
4	More than three cracks. Cleaves at two indentation sides
5	Complete indentation shape destruction

Tracking the development of cracks during microindentation of a langatate crystal and evaluating its brittleness one can conclude that the brittleness of the material starts to show itself at a 5 g load. These results suggested that Vickers microhardness testing of langatate crystals requires loads of within 3 g.

The effect of growth atmosphere on langatate microhardness was studied for a 3 g indenter load. Figure 3 shows photos of indentations on Y cuts with different polarities at different plate sides (+) and (–) and Z cuts of crystals grown in an Ar + < 2 % O_2 atmosphere. Table 3 shows measurement results for a 3 g load.

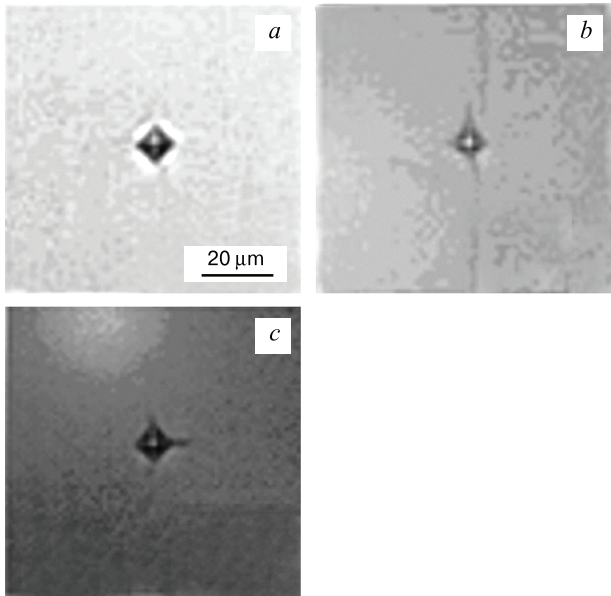


Figure 3. Indentations in langatate crystal grown in an Ar + < 2 % O₂ atmosphere for 3 g load: (a) Y cut (+), (b) Y cut (-) and (c) Z cut

Table 3. Effect of growth atmosphere on langatate crystal microhardness.

Growth atmosphere	Microhardness, GPa	
	+	-
Ar + 2 % O ₂	6.5 ± 5 %	7.7 ± 5 %
Ar + < 2 % O ₂	6.5 ± 5 %	7.0 ± 5 %
Ar	5.9 ± 5 %	7.4 ± 5 %
Air	6.5 ± 5 %	7.7 ± 5 %

Table 4 shows comparative microhardness measurement data for Z and Y cut langatate crystal specimens grown in an Ar + < 2 % O₂ atmosphere, indenter load 3 g.

Table 4. Langatate crystal microhardness measurement data (growth atmosphere Ar + < 2 % O₂) for different cuts.

Cut	3 g load microhardness, GPa
	3 g
Y cut (+)	6.5 ± 5 %
Y cut (-)	7.0 ± 5 %
Z cut	5.9 ± 5 %

Thus Vickers microhardness measurements show langatate crystal microhardness to depend on growth atmosphere. Crystals grown in an oxygen containing atmosphere have a higher microhardness than those grown in an argon atmosphere. Langatate crystal microhardness exhibits anisotropy regardless of growth atmosphere: the microhardness of positive polarity sides for polar cuts is lower than that of negative polarity sides, the Z cut having the lowest microhardness.

Since langatate crystals are brittle (Fig. 3) and hence microhardness testing can hardly give authentic results, we conducted an II study for the same specimens at a test load of 10 mN and a load rate of 0.33 mN/s. The test error was within 1% for hardness, 3% for elastic modulus and 10% for elastic recovery. Each specimen was indented for

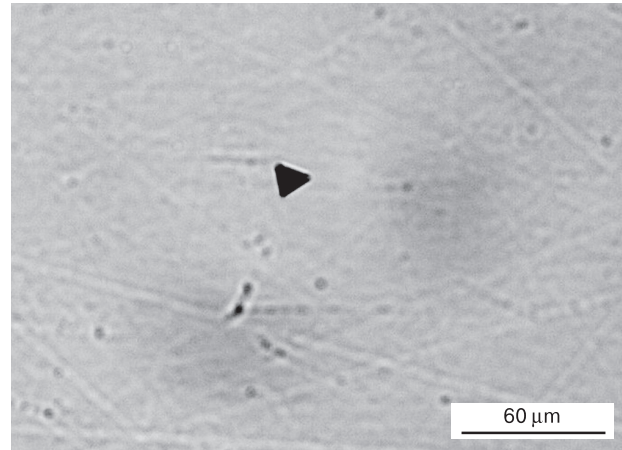


Figure 4. Appearance of Berkovich indentation in Y cut (-) langatate crystal specimen grown in an argon atmosphere

10 times. Figure 4 shows indentation appearance for the Y cut langatate specimen (-) grown in an argon atmosphere.

The II test results (Table 5) suggest that the hardness, elastic modulus and elastic recovery coefficient of langatate crystals depend on growth atmosphere: crystals grown in an oxygen containing atmosphere had higher parameters compared with those grown in an argon atmosphere.

Table 5. Mechanical properties data obtained by instrumented indentation for langatate crystals, grown at different conditions.

Growth atmosphere	Hardness, GPa		Elastic modulus, GPa		Elastic recovery coefficient, %	
	+	-	+	-	+	-
Ar	10.7 ± 1%	11.0 ± 1%	142 ± 3%	143 ± 3%	39 ± 10%	40 ± 10%
Ar + < 2% O ₂	11.9 ± 1%	12.1 ± 1%	147 ± 3%	148 ± 3%	41 ± 10%	41 ± 10%
Air	12.1 ± 1%	12.6 ± 1%	146 ± 3%	147 ± 3%	42 ± 10%	43 ± 10%
Ar + 2% O ₂	12.0 ± 1%	12.0 ± 1%	146 ± 3%	148 ± 3%	42 ± 10%	42 ± 10%

II results on anisotropy of mechanical properties in langatate crystals are summarized in Table 6. The results show that the Y and Z cut langatate crystals exhibit strong anisotropy of elastic modulus and elastic recovery coefficient.

Table 6. Mechanical properties data obtained by instrumental indentation for different cuts of langatate crystals grown in an Ar + < 2 % O₂ atmosphere.

Cut	Hardness, GPa	Young's modulus, GPa	Elastic recovery coefficient, %
Y cut (+)	11.9 ± 1 %	147 ± 3 %	41 ± 10 %
Y cut (-)	12.6 ± 1 %	146 ± 3 %	41 ± 10 %
Z cut	12.1 ± 1 %	183 ± 3 %	35 ± 10 %

The results confirm the conclusions made for Vickers hardness tests: the hardness of positive polarity cuts is lower than that of negative ones. The difference between the Vickers and II hardness data can be accounted for the possible reasons: either the cracks occur, but not visible, or the surface layer is harder than the deep layer due to the polishing characteristics. Thus, this requires further research.

5. Conclusion

The brittleness of langatate crystals manifests itself at loads of 5 g and higher regardless of crystal growth atmosphere.

Growth atmosphere has an effect on the mechanical properties of langatate. The microhardness, hardness, elastic modulus and elastic recovery coefficient are higher for crystals grown in an oxygen containing atmosphere.

The microhardness of polar *Y* cut langatate crystals exhibits anisotropy. The microhardness, hardness and elastic modulus of the positive polarized side of *Y* cut is

lower than for negative one. The microhardness of *Y* cut langatate crystal is higher than that of *Z* cut one.

Instrumented indentation data suggest that *Z* and *Y* cut langatate crystals grown in argon with less than two percent oxygen exhibit strong elastic modulus and elastic recovery coefficient anisotropy.

Acknowledgements

The Authors are grateful to JSC Fomos-Materials and Oleg A. Buzanov for providing lanthanum-gallium tantalate crystals.

References

- Grinev B. V., Dubovik M. F., Tolmachev A. V. *Opticheskie monokristally slozhnykh oksidnykh soedinenii* [Optical monocrystals of complex oxide compounds]. Kharkov: Institut monokristallov, 2002: 252. (In Russ.)
- Kaminsky A. A. *Fizika i spektroskopiya lazernykh kristallov* [Physics and spectroscopy of laser crystals]. Moscow: Nauka, 1986: 271. (In Russ.)
- Mill B. V., Maksimov B. A., Pisarevsky Yu. V., Danilova N. P., Markina M. P., Pavlovskaya A., Werner S., Schneider J. Phase transitions in langasite family crystals. *Proc. IEEE International Frequency Control Symposium and Exposition*, 2004: 52–60. <https://doi.org/10.1109/FREQ.2004.1418428>
- Zhang S., Yu F. Piezoelectric materials for high temperature sensors. *J. Am. Ceram. Soc.*, 2011; 94(10): 3153–3170. <https://doi.org/10.1111/j.1551-2916.2011.04792.x>
- Yu F. P., Chen F. F., Hou S., Wang H. W., Wang Y. A., Tian S. W., Jiang C., Li Y. L., Cheng X. F., Zhao X. High temperature piezoelectric single crystals: Recent developments. *Proc. Symposium on Piezoelectricity, Acoustic Waves, and Device Applications (SPAWDA)*, 2016. <https://doi.org/10.1109/SPAWDA.2016.7829944>
- Nehari A., Alombert-Goget G., Benamara O., Cabane H., Dumortier M., Jeandel P., Lasludji I., Mokhtari F., Baron T., Wong G., Allani M., Boy J., Alzuaga S., Arapan L., Gegot F., Dufar T., Lebbou K. Czochralski crystal growth and characterization of large langatate ($\text{La}_3\text{Ga}_{5.5}\text{Ta}_{0.5}\text{O}_{14}$, LGT) crystals for SAW applications. *CrystrEngComm.*, 2019; 21(11): 1764–1771. <https://doi.org/10.1039/C8CE02157K>
- Takeda H., Tanaka S., Izukawa S., Shimizu H., Nishida T., Shiosaki T. Effective substitution of aluminum for gallium in langasite-type crystals for a pressure sensor use at high temperature. *IEEE Ultrasonics Symposium*, 2005: 560–563. <https://doi.org/10.1109/ULTSYM.2005.1602915>
- Kuz'Micheva G.M., Tyunina E.A., Kaurova I.A., Domoroshchina E.N., Zaharko O., Rybakov V. B., Dubovsky A. B. Point defects in langatate crystals. *Crystallogr. Rep.*, 2009; 54(2): 279–282. <https://doi.org/10.1134/S1063774509020163>
- Kugaenko O.M., Torshina E.S., Petrakov V.S., Buzanov O.A., Sakharov S.A. Anisotropy of Microhardness Crystals of the Langasite Family. *Izvestiya Vysshikh Uchebnykh Zavedenii. Materialy Elektronnoi Tekhniki = Materials of Electronics Engineering*, 2014; (3): 174–182. (In Russ.). <https://doi.org/10.17073/1609-3577-2014-3-174-182>
- Kugaenko O.M., Torshina E.S., Buzanov O.A., Sakharov S.A. Anisotropy of microhardness and resistance to cracking for crystals of the langasite family. *Bull. Russ. Acad. Sci. Phys.*, 2014; 78(11): 1188–1196. <https://doi.org/10.3103/S106287381411015X>
- Kugaenko O.M., Uvarova S.S., Petrakov V.S., Buzanov O.A., Egorov V.N., Sakharov S.A., Pozdnyakov M.L. Plastic deformation of piezoelectric lanthanum-gallium tantalate crystals during cyclic mechanical actions. *Russ. Metall.*, 2013; 2013(4): 286–291. <https://doi.org/10.1134/S0036029513040071>
- Buzanov O.A., Zabelina E.V., Kozlova N.S. Optical properties of lanthanum-gallium tantalate at different growth and post-growth treatment conditions. *Crystallogr. Rep.*, 2007; 52(4): 691–696. <https://doi.org/10.1134/S1063774507040177>
- Zabelina E.V. Inhomogeneities in crystals of lanthanum-gallium tantalate and their effect on optical properties. Diss. Cand. Sci. (Phys.-Math.). Moscow, 2018: 150. (In Russ.)
- Boursier E., Segonds P., Boulanger B., Félix C., Debray J., Jegouso D., Ménaert B., Roshchupkin D., Shoji I. Phase-matching directions, refined Sellmeier equations and second-order nonlinear coefficient of the infrared langatate crystals $\text{La}_3\text{Ga}_{5.5}\text{Ta}_{0.5}\text{O}_{14}$. *Opt. Lett.*, 2014; 39(13): 4033–4036. <https://doi.org/10.1364/OL.39.004033>
- Boutahraoui B., Nehari A., Boy J., Vacheret X., Allani M., Cabane H., Dumortier M., Derbal M., Lebbou K. LGT ($\text{La}_3\text{Ga}_{5.5}\text{Ta}_{0.5}\text{O}_{14}$) langatate bulk crystal grown from the melt by Czochralski technique and characterization. *Opt. Mater.*, 2017; 65: 103–105. <https://doi.org/10.1016/j.optmat.2016.09.018>
- Kawanaka H., Takeda H., Shimamura K., Fukuda T. Growth and characterization of $\text{La}_3\text{Ta}_{0.5}\text{Ga}_{5.5}\text{O}_{14}$ single crystals. *J. Crystal Growth*, 1998; 183(1–2): 274–277. [https://doi.org/10.1016/S0022-0248\(97\)00481-8](https://doi.org/10.1016/S0022-0248(97)00481-8)
- Alani M., Batis N., Laroche T., Nehari A., Cabane H., Lebbou K., Boy J.J. Influence of the growth and annealing atmosphere on the electrical conductivity of LGT crystals. *Opt. Mater.*, 2017; 65: 99–102. <https://doi.org/10.1016/j.optmat.2016.09.072>
- Buzanov O.A., Zabelina E.V., Kozlova N.S., Sagalova T.B. Near-electrode processes in lanthanum-gallium tantalate crystals. *Crystallogr. Rep.*, 2008; 53(5): 853–857. <https://doi.org/10.1134/S1063774508050210>

19. Musil J., Zeman H., Kunc F., Vlček J. Measurement of hardness of superhard films by microindentation. *Mater. Sci. Eng. A*, 2003; 340(1–2): 281–285. [https://doi.org/10.1016/S0921-5093\(02\)00194-6](https://doi.org/10.1016/S0921-5093(02)00194-6)
20. Veprek S., Mukherjee S., Männling H.-D., He Jianli. On the reliability of the measurements of mechanical properties of superhard coatings. *Mater. Sci. Eng. A*, 2003. 340(1–2): 292–297. [https://doi.org/10.1016/S0921-5093\(02\)00195-8](https://doi.org/10.1016/S0921-5093(02)00195-8)
21. Zolotarevsky V.S. *Mekhanicheskie svoystva metallov* [Mechanical properties of metals]. Moscow: MISiS, 1998: 400. (In Russ.)
22. Hertz H. R. Über die Berührung fester elastischer Körper. *J. für die reine und angewandte mathematik*, 1882; 92: 156–171. <https://doi.org/10.1515/crll.1882.92.156>
23. Landau L., Lifshitz M. *Teoriya uprugosti* [Theory of Elasticity]. Moscow: Nauka, 1987: 248. (In Russ.)
24. GOST 2999-75. *Metally i splavy. Metod izmereniya tverdosti po Vickersu* [Metals and alloys. Vickers hardness measurement method]. Moscow: Izd-vo standartov, 1986. (In Russ.)
25. Petrzhik M.I., Levashov E.A. Modern methods for investigating functional surfaces of advanced materials by mechanical contact testing. *Crystallogr. Rep.*, 2007; 52(6): 966–974. <https://doi.org/10.1134/S1063774507060065>
26. Golovin Yu.I. Nanoindentation and mechanical properties of materials in the submicro- and nanoscale. Recent results and achievements (Review). *Fizika tverdogo tela = Physics of the Solid State*, 2021. 63(1): 3–42. (In Russ.). <https://doi.org/10.21883/FTT.2021.01.50395.171>
27. ASTM Designation E2546-15 Standard Practice for Instrumented Indentation Testing.
28. Glazov V.M., Vigdorovich V.N. *Mikrotverdot' metallov* [Microhardness of Metals]. Moscow: Metallurgizdat, 1962: 11–48. (In Russ.)